38th International Electric Vehicle Symposium and Exhibition (EVS38) Göteborg, Sweden, June 15-18, 2025

Concept: Minimization of Testing Effort at Battery System Level by Simulation

Tobias Brehler, Claudius Diez, Markus Lienkamp
Technical University of Munich (TUM), School of Engineering & Design, Department of Mobility Systems Engineering, Institute of Automotive Technology, tobias.brehler@tum.de

Executive Summary

Battery aging depends significantly on the operating conditions. Since these differ from cell to cell in connected systems, examining aging at the cell level is not sufficient. Lifetime tests at the system level are expensive and time-consuming due to their high complexity. In this work, a holistic concept is presented to model batteries at the system level to decrease experimental testing effort: All components from the equivalent circuit and lumped thermal cell model with integrated semi-empirical aging model to the system model are incorporated. The electrical and thermal parameterization for each model are included. The validation is carried out with commercial cells and self-built modules.

Keywords: *Batteries, Modelling and Simulation, Measuring Methods & Equipment, Digital Twin Design Tools, Electric Vehicles*

1 Introduction

The deployment of Lithium-ion batteries as energy storage in battery electric vehicles (BEV) is state of the art [1]. Among other factors, the operating conditions of the battery contribute significantly to the aging process, i.e., the deterioration of the parameters such as the decrease in capacity and the increase in internal resistance, and thus loss in driving range and available power. In order to meet the requirements for battery service life, a wide range of conditions is tested as multiple stress factors such as (dis-)charging rates, cycle depth and temperature significantly influence battery aging. These tests take from a few days to several years [2], depending on the conditions and cell chemistry, and are therefore time-consuming and costly. It is common practice to minimize the number of tests required by design of experiment [3] and the duration by accelerated life testing [2].

In BEVs, cells are connected in series and usually parallel to meet the requirements for power and range. The statuses of the cells (e.g., state of charge, health, safety) in a real system differ, among other things, in terms of the individual current load and temperature due to, for example, production fluctuations in cell production [4–13], varying contact resistances [14–20] and unequal thermal boundary conditions [11, 12, 21, 22]. Therefore, additional life cycle tests are carried out at system level. Compared to cell-level tests, system-level tests are more expensive for two reasons: Firstly, the required currents and voltages are significantly higher necessitating high-price testing equipment. Secondly, additional peripherals such as a battery management system and often a thermal management system are necessary. Taking into account the large number of test specimen required across the various sample statuses in a series development in the automotive industry, this results in considerable costs. The time needed for testing at the system level is comparable to that at the cell level ($\gtrsim 1$ year [2]). However, testing at the system level usually does not begin until the cell tests have been completed. This extends the development process and drives up the costs.

Complementary to the experiments, the modeling of such systems is a promising subject of current research. The subsequent section outlines the state of the art: Lucero et al. [23] introduce a battery pack model based on a first order equivalent circuit model (ECM) with a lumped thermal model and semi-empirical aging model (SEAM) for the capacity and ohmic resistance. The deterioration of the RC parameters and the OCV as well as the current dependence are neglected. Furthermore, the validation is lacking, as only one electrical point of operation is tested on cell and system level making any interpolation of the SEAM unnecessary. This concept is similar to that of Cordoba-Arenas et al. [24] with a first order ECM, lumped thermal mass and aging of capacity as well as ohmic resistance; the model of Cordoba-Arenas et al. is not validated. Escobar et al. [25] employ an ECM without RC elements and a lumped thermal model combined with aging models for the capacity and resistance based on the Arrhenius equation; the electrical and the aging model are not validated. Gálik et al. [26] focus on the thermal behavior on system level and disregard aging; the model is also based on a first order ECM and a lumped thermal mass on cell level. Jaguemont et al. [27] follow a similar approach with one RC element and a lumped thermal mass neglecting aging. Kolmbauer et al. [28] developed a method to scale efficiently from cell to system level; it is not linked to specific electrical or thermal models. He et al. [29], Neupert et al. [30] and Reiter et al. [31] place a greater focus on the electrical modeling with two and four RC elements respectively but disobey aging within their models.

In the vast majority of state-of-the-art system models, the individual cells are modeled with ECMs, since these offer sufficient accuracy for many investigations with acceptable parameterization effort [32]. In previous studies, only the parameters cell capacity and ohmic resistance are adjusted as a function of aging during system modeling, but not the dynamic RC parameters. This results in a decreasing simulation accuracy in dynamic operation with increasing aging. Furthermore, the convergence of the ECM might no longer be guaranteed if some components of the voltage response are adjusted (e.g., by deteriorating the ohmic resistance) and others are not (e.g., by not adapting the parameters of the RC elements).

In order to accelerate the development process and to reduce the costs for the tests and test specimen, this article presents a novel concept for modeling battery systems. The concept includes a cell and a modular system model, the electrical and thermal parameterization of the models, and the modeling of the aging behavior without the need to experimentally cycle battery systems. The objective of this study is to design a model that achieves a high level of accuracy with minimal and straightforward measurement requirements for parameterization.

2 Methodology

Due to the trade-off between parameterization effort and model accuracy, an ECM and a lumped thermal model are used at the cell level. These models are extended by a semi-empirical aging model that takes into account the degradation of capacity and resistance as well as the degradation of the dynamic resistance parameters.

The cell model and its parameterization are described below. The implementation is carried out in Simscape Battery (MATLAB Simulink), which provides a basic structure for an ECM including a thermal sub model [33]. The investigations by Reiter et al. [31] showed that the use of two RC elements provides the best compromise between accuracy and computational effort. The underlying equations describing the electrical behavior are listed below. The dynamic parameters R_n as well as C_n depend on the state of charge (SoC), the current directionality and the temperature (T). The open circuit voltage (OCV) is a function of the SoC. The employed one state model according to Plett [34] incorporates the hysteresis behavior of the battery. The difference between charge and discharge pOCV curve can be interpreted as maximum hysteresis voltage at the respective SoC.

$$U_k = U_{OCV} + U_{R0} + U_{RC1} + U_{RC2} \tag{2.1}$$

$$U_{R0} = R_0 I \tag{2.2}$$

$$U_{RCn} = R_n I \left(1 - e^{-\Delta t / R_n C_n}\right) \tag{2.3}$$

In order to parametrize the electrical model, three tests are conducted within our Reference Performance Tests (RPT):

- A C/3 discharge after a CC-CV (C/20 at 4.2 V) charge to determine the capacity
- A C/10 partial OCV charge and discharge to average the OCV
- A hybrid pulse power characterization (HPPC) with 1 C pulses in both charge and discharge direction to calculate the dynamic parameters. The RC parameters are determined by means of the numerical optimization according to Baumann [35].

The cylindrical cells were contacted by Arbin Instruments 30A/60A battery holders. A BioLogic SAS BCS-815 (0-9V, 15A) and a BaSyTec XCTS25 (0-6V, 25A) measurement device were used. To ensure constant and comparable climatic ambient conditions, a Binder KB400 and a Vötsch VC³ 4100 thermal chambers were employed.

Irreversible heat generation (i.e., dissipated power) and reversible heat generation can be taken into account within the thermal model; this work only considers irreversible heat generation as reversible heat plays a subordinate role at the regarded C-rates [36]. The resulting temperature is calculated by comparing the difference between generated heat within the cell and heat transport across the cell boundary with the temperature change and the lumped thermal mass (m_{th}) of the cell. The governing equations are listed in the following:

$$\dot{Q}_{gen} = \dot{Q}_{irrev} + \dot{Q}_{rev} \tag{2.4}$$

$$\dot{Q}_{irrev} = R_0 I^2 + U_{RC1} I + U_{RC2} I \tag{2.5}$$

$$\dot{Q}_{rev} = I\,T\frac{dU}{dt} \tag{2.6}$$

$$m_{th}\frac{dT}{dt} = \dot{Q}_{gen} - \dot{Q}_{diss} \tag{2.7}$$

The heat transport ($\dot{Q}_{diss}$) can be written as temperature delta over cumulated thermal resistance. Thus, two parameters need to be determined: the thermal mass (consisting of specific heat capacity and gravimetric mass) and the cumulated thermal resistance. The specific heat capacity as well as the thermal resistance were determined by utilizing the method of Bryden et al. [37]: The cell is heated up twice by applying an alternating current until it reaches a steady state temperature. Two convective boundary conditions are applied: Natural and forced convection; for the latter, a controllable fan is employed. The experimental setup is illustrated in Figure 1.

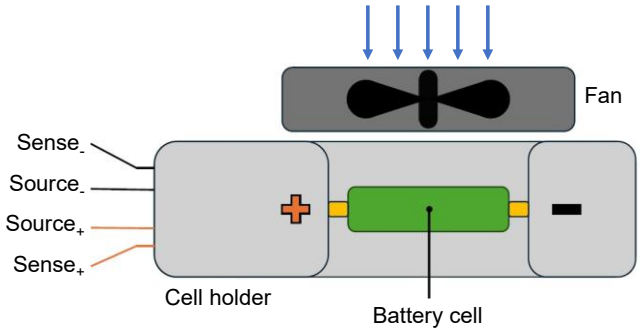

Figure 1: Experimental setup to parametrize the thermal model

The Battery Builder app from Simscape Battery [33] is employed for the cell-to-system scaling. It contains different assembly stages: Single cells are first connected to parallel assemblies which can be connected in series to build modules. Furthermore, module assemblies and packs are feasible by stacking the underlying stage in series. The stages up to module assembly are utilized in this work. Cylindrical cells can be positioned in two ways: Either in a square or in a hexagonal topology. Although the latter is common in today's vehicles [38] as of the increased energy density on system level, the former is chosen in this work because of the space requirements for the temperature sensors in between the cells. The cell-to-cell distance is set to 2.5 mm. To parametrize the thermal boundaries against the ambience, a vector with the thermal resistance for each cell is specified. These thermal resistance values consider conduction, convection, and radiation. They're evaluated by fitting the simulated temperature response to the measured. The cell-to-cell heat exchange is assumed to be negligible.

Simscape Battery [33] offers a cycling aging model that can be linked to the electro-thermal cell model. It models the decrease of the capacity and the increase of all resistances by using a square root correlation linking two (or more) measurement points, e.g., the parameters at begin of life (BoL) and end of life (EoL). The model neglects the change in capacitance of the RC elements and is limited to square root correlations. The most critical limitation is the restriction to one stress factor: the temperature. Other stress factors like the depth of discharge (DoD) are not considered. The consideration of the DoD is of high importance when scaling to system level to model the impact of diverging cell capacities: Cell-to-cell variations, differing contact resistances and thermal gradients lead to inhomogeneous cell states [39], e.g., state of charge and state of health. Therefore, the authors developed and integrated a novel aging model. The SEAM according to Kröger et al. [3] serves as the basis. This model provides good results for the capacity decrease of the cells, taking into account the stress factors cell temperature, charging rate and depth of discharge. The training of the capacity SEAM is done in accordance to the cited article with a D-optimal test plan; the validation cells are used to validate the model. For the modeling of the dynamic parameters, the underlying equation is simplified (equation (2.9)) as the charging rate is not altered within this study.

$$SoH_R = 1 + \beta\, Q^{\alpha} \tag{2.8}$$

$$\beta = \ln\left(\beta_0 + \beta_T \frac{1}{T} + \beta_{DoD} DoD + \beta_{T,DoD} \frac{DoD}{T} + \beta_{T^2} \frac{1}{T^2} + \beta_{DoD^2} DoD^2\right) \tag{2.9}$$

For the parametrization of the SEAM for the dynamic parameters (i.e., R_0, R_1, R_2), all cells with 2C/3 charge current are selected from the underlying dataset [3], to serve as reference and consider the two stress factors temperature and depth of discharge while having the same charge rate. One SEAM for both current directions is chosen as the mean absolute percentage error (MAPE) is less than 1 % higher but the complexity lower. As a starting point, there is one SEAM for all SoCs. The degradation at 50 % SoC is used as reference.

The concept is validated using a commercial cylindrical cell (LG Chem INR 18650 MJ1). An aging study at the cell level has already been published for the cylindrical cell [3]. This dataset provides the basis for the aging model (parametrization as well as validation). In order to examine the influences due to the interconnection topology (1s16p, 16s1p, 4s4p) and the spatial arrangement (2x8, 4x4, see Figure 2), a total of six laser-welded modules, each consisting of 16 MJ1 cells, are cycled under same conditions. Each cell is equipped with a temperature sensor so that thermal influences can be investigated. The modules in 2x8 topology are depicted in Figure 3. To build the modules, 100 pristine MJ1 cells were procured and 96 cells were used to build the six modules with 16 cells each (random cell selection). The complete set of 100 cells serves as reference for the parametrization of the models at BoL.

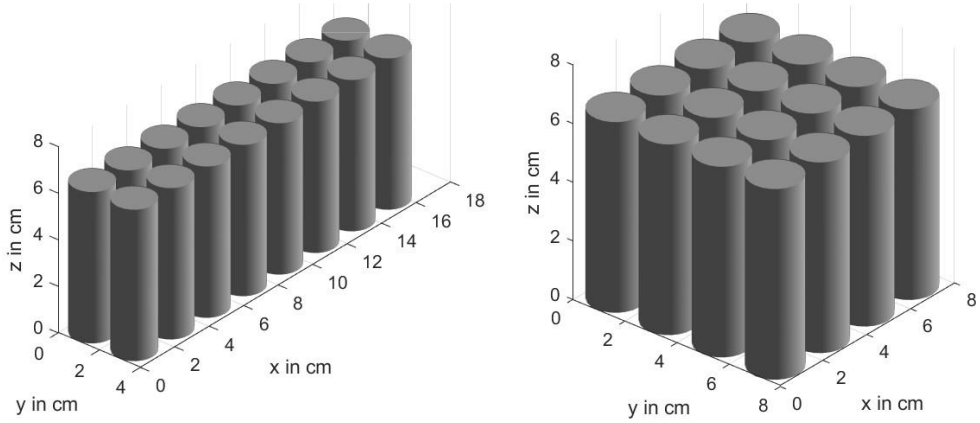

Figure 2: Modules in spatial 2x8 and 4x4 arrangement (generated with Simscape Battery)

Figure 3: Assembled modules in 2x8 topology (1s16p, 16s1p, 4s4p)

The following stress factors are selected as test conditions at system level because this stress has led to an aging trajectory with knee point at the cell level: A DoD of 55 % around 50 % mean SoC (i.e., cycling between 22.5 and 77.5 % SoC) with 1 C discharge and 2/3 C charge current at 20 °C ambient temperature. There is no rest in between the cycles. RPTs are performed every five days and include a C/3 capacity determination, a C/10 pOCV charge and discharge as well as an HPPC test including 1 C current pulses in both charge and discharge direction and 10 % SoC steps. The tests are conducted with Keysight Scienlab test devices. As the aging tests on system level are still ongoing, the validation within this work will be limited to the BoL. The aging on module level is to be validated in an upcoming work. The validation is carried out on the spatial 2x8 arrangement, as there is no data for every configuration yet (experimental tests are ongoing). All three topologies are compared regarding their electrical and thermal behavior.

3 Results

In the following, the results of the model parametrization are described, beginning with the electrical model. The mean capacity is determined to 3.349 Ah with 0.014 Ah standard deviation and 0.43 % coefficient of variation, based on a reference set of 100 pristine cells prior to module assembly. The cell spread is considered by means of a vector that assigns the actual spread referring to the mean capacity (i.e., measured capacity at BoL / mean capacity at BoL) towards the cells in each module. The OCV is the mean of the pOCV charge and discharge curves (Figure 4). Especially below 15 % SoC an increased hysteresis is apparent.

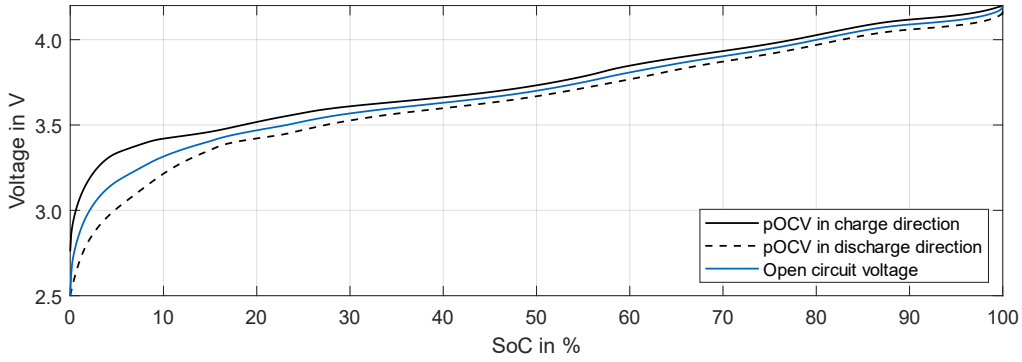

Figure 4: Open circuit voltage as mean of charge and discharge pOCV

The number of employed RC elements has a significant impact on the ability to model the voltage response of the battery under a 1 C current pulse (Figure 5): The maximum error is 12.64 mV with one RC element and 1.63 mV with 2 RC elements. Further increasing the number of RC elements does not result in a comparable improvement as the error with four RC elements is 0.65 mV.

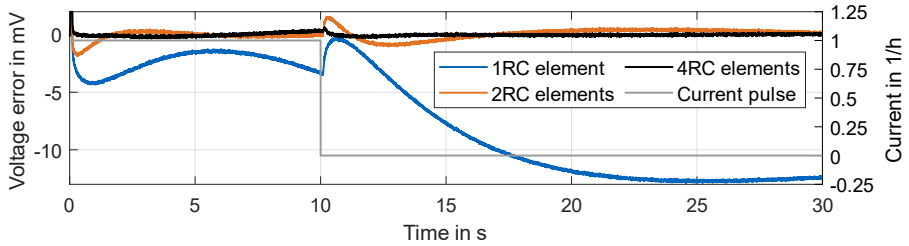

Figure 5: Pulse fitting error: 2 RC elements with best trade-off between error and complexity

The calculated RC parameters for all 100 cells (before assembly) at BoL are shown for 25, 50 and, 75 % SoC (Figure 6). An SoC dependence of all parameters can be seen while a current directionality dependence is not apparent. Therefore, the current dependence is neglected in the following and the discharge data is used. The time constant for the first RC element is close to one second; thus, the solver time should be at least one second or smaller.

As described in section 2, the thermal characterization was implemented according to Bryden et al. [37]. The determined specific heat capacity is 927.5 J kg^{-1} K^{-1} with a gravimetric cell mass of 47 g. The thermal resistance is 7.5 K W^{-1} under natural convection and 3.9 K W^{-1} under forced convection with regards to the cell surface.

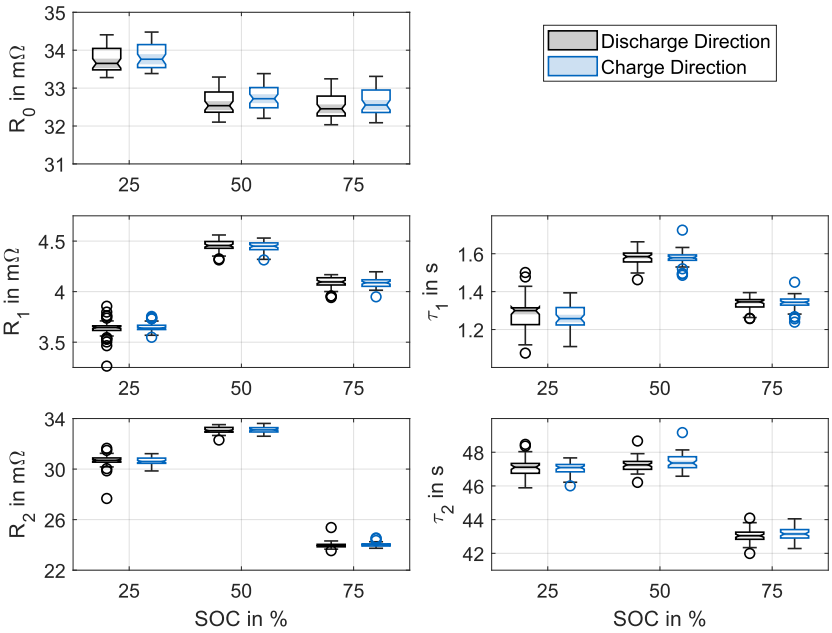

Figure 6: Overview of determined RC parameters according to Baumann [35]
Parameters show significant SoC dependence but no current directionality dependence

Next, the results of the semi-empirical aging model are shown for all nine cells that were used to train the model (Figure 7). Each subplot contains measurements and fitted data for one cell. The subplots are sorted by DoD (columns) and ambient temperature (rows) and contain capacity as well as resistances. The measurement data is indicated by symbols, the fitted SEAMs by line plots in the same color. This visualization emphasizes the damaging effect of DoD as stress factor on all parameters. Higher temperatures reduce the stress and thus the aging of the battery. The implemented SEAMs can model the aging behavior under moderate stress but struggle at low temperatures. The deterioration of all parameters is overestimated at 10 °C ambient temperature, especially at 55 % DoD.

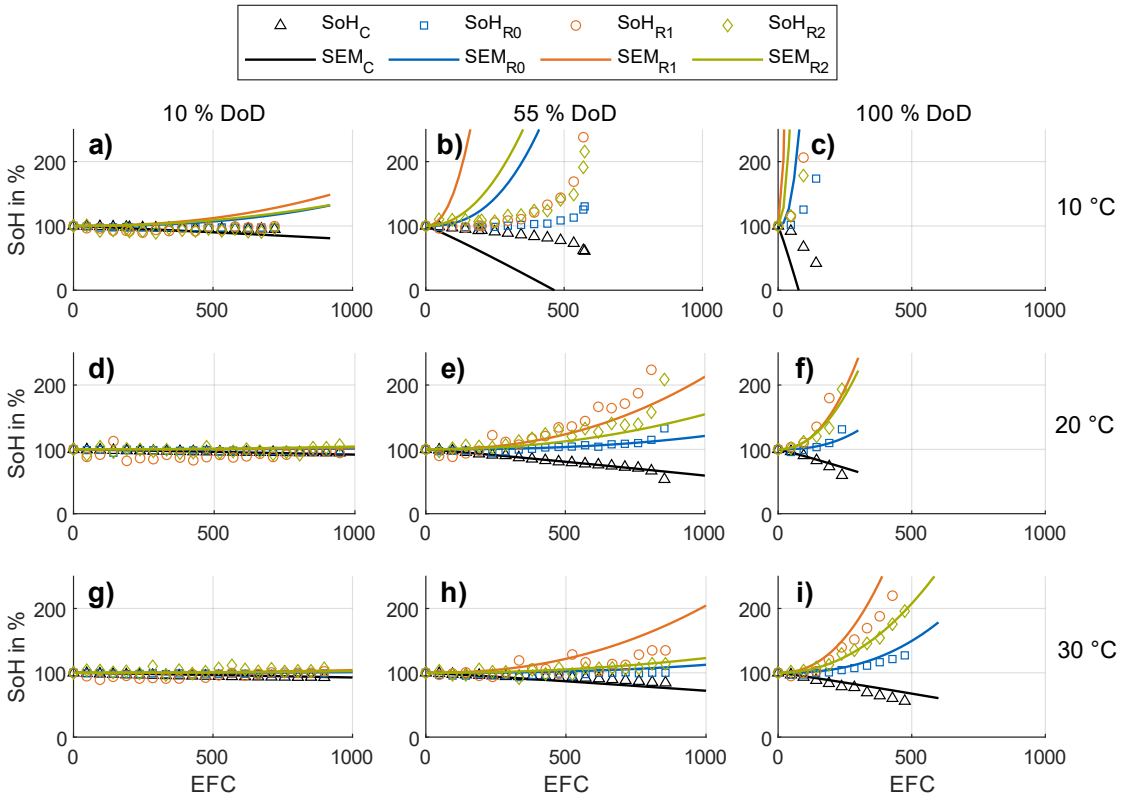

Figure 7: Semi-empirical aging models for capacity loss as well as $R_{0,1,2}$ increase for all cells a) – i)

Two error metrics are deployed: the MAPE as well as the root mean squared error (RMSE). The commonly used coefficient of determination (R^2) is not used as it is unable to capture the fit quality on a diverse dataset by virtue of its underlying formula. For all parameters the MAPE is below 10 %.

Table 1: Error metrics of the semi-empirical aging models

	C	R_0	R_1	R_2
MAPE in %	7.1	2.3	9.1	4.8
RMSE in %	7.9	3.6	18.9	7.9

The validation of the electro-thermal cell model including the aging models is depicted in Figure 8. For the full trajectory until the end of test, the RMSE is 5.7 % and the MAPE 5.6 %. Typical end-of-life criterions in BEV applications are 70-80 % state of health. Up to that point, the RMSE and MAPE are significantly lower with 2.2 % and 1.9 % at 80 % SoH and 3.2 % and 3.4 % at 70 % SoH. The SEAM is unable to model the knee point occurring at 800 EFC, resulting in increased errors after 750 EFC.

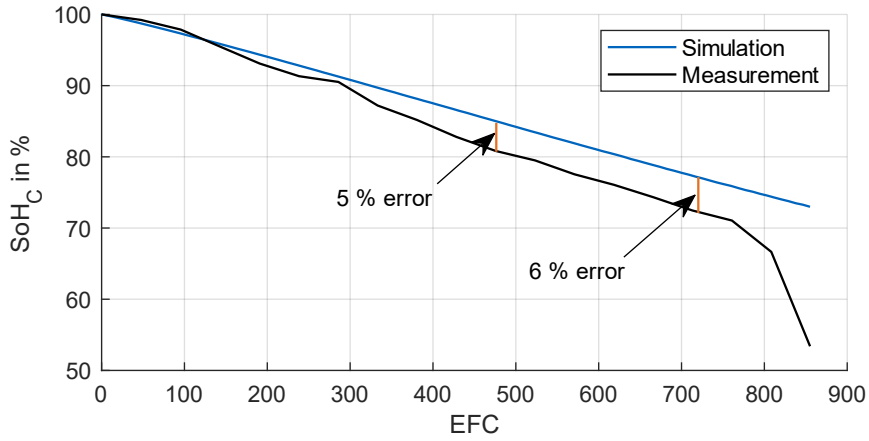

Figure 8: Validation of capacity loss during cyclic aging
1.9 % and 3.4 % MAPE up to 70 % and 80 % SoH respectively; unable of modeling knee point

The results of the validation of the electrical and thermal models on system level are shown below. For reasons of brevity, only the most complex electrical topology (4s4p) of the three examples (Figure 3) is visualized here. The performance metrics for the two remaining topologies are given nonetheless. The chosen error metrics (MAPE and RMSE) are calculated over the first four cycles to account for the process of becoming quasi-stationary. As explained in section two, only the spatial 2x8 configurations are validated as the 4x4 systems are still under test.

In general, the simulation captures the electric real-world behavior accurately according to Figure 9. The MAPE and RMSE regarding system voltage with 0.60 % and 0.12 V, respectively, confirm that. Especially the charge phases are simulated with high precision and errors below 150 mV. When reaching medium SoC, the model loses accuracy during discharge phases and the error rises to almost 400 mV – what translates to 100 mV on cell level. Furthermore, the ECM struggles with low SoCs owing to the increased hysteresis below 3.5 V (on cell level). The fidelity of the simulation is similar for the two other electrical topologies: The MAPE is 0.55 % for the 1s16p configuration and 0.60 % for the 16s1p topology. The RMSE scales proportionately to the number of cells connected in series: It results in 0.03 V for the pure parallel connection and 0.48 V for the pure serial connection.

The simulation enables investigating another aspect that cannot be validated without additional measurement equipment: the current distribution between cells connected in parallel. As introduced in section one, several reasons lead to inhomogeneous currents within parallel connections. The simulated currents for one of the four 4p connections are depicted in Figure 10. Interestingly, two of the four cells are exposed to the identical cell current. In accordance with the literature [40], the current distribution is not static but changes during the charging and discharging phases.

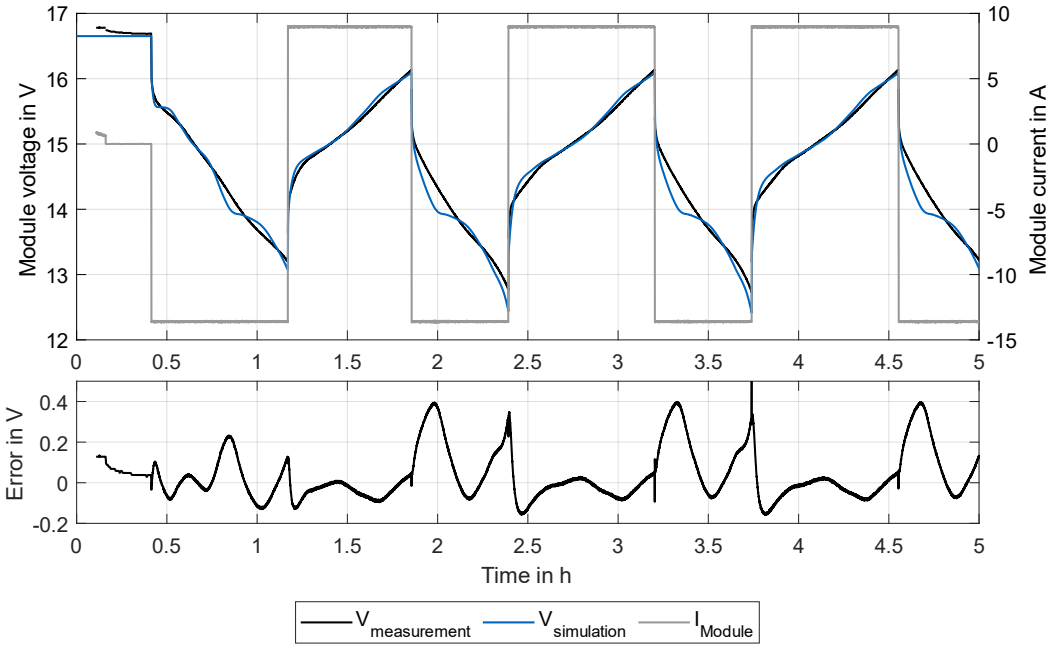

Figure 9: Electric validation of the 4s4p module in 2x8 arrangement
0.60 % MAPE and 120 mV RMSE at system level voltage

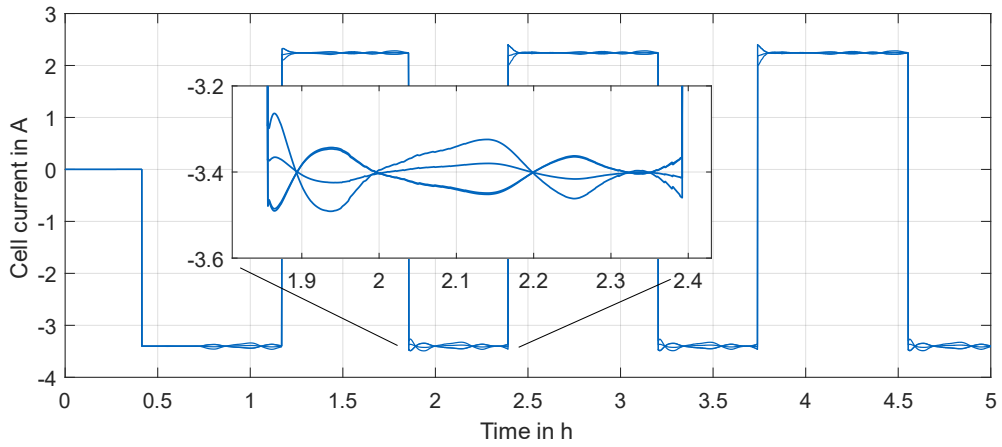

Figure 10: Current distribution within first 4p parallel connection
Two out of four parallel cells are exposed to the identical current.

In the following, the cell temperatures are examined. Comparing the cell temperature curves with the current, it is evident that the cells are getting warmer during discharging than charging. This originates from the higher currents when discharging in combination with similar resistance parameters in both current directions. Within the simulation, the hottest cells almost reach 45 °C, while in the validation measurement all cells stay below 42 °C during the first cycles. The error metrics are calculated between the mean of all simulated and all measured cell temperatures which are depicted in Figure 11. This results in an MAPE of 5.37 % and an RMSE of 2.18 °C for the 4s4p topology. For both remaining topologies, the errors are comparable: The MAPE is 5.72 % and the RMSE 2.20 °C for the 1s16p module, while the respective metrics are 4.91 % and 1.89 °C for the 16s1p topology.

Below in Figure 12, the simulated 4s4p module in 2x8 topology is depicted to visualize the temperature spread within the module at the maximum temperature (time = 145 min). As expected, the cells in the middle of the module experience higher temperatures than the cells at the ends with cells only on two but not three sides.

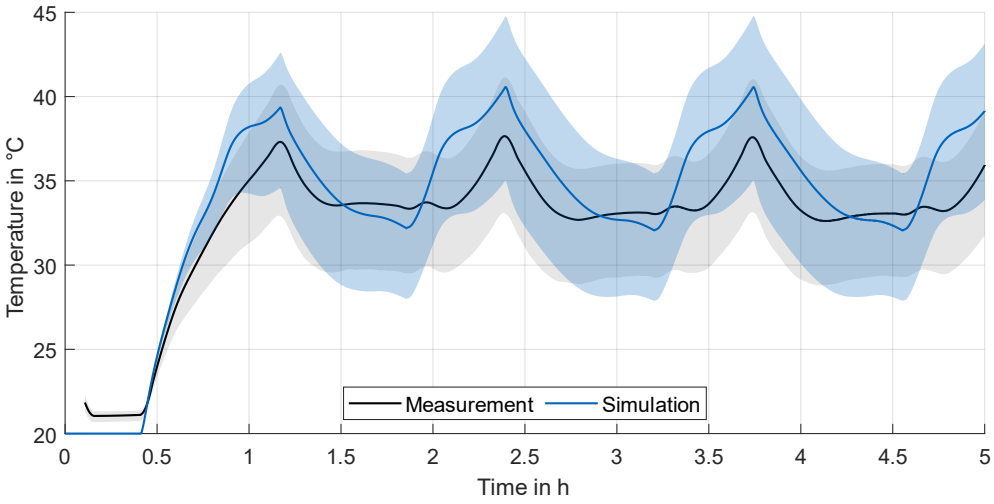

Figure 11: Thermal validation of the 4s4p module in 2x8 arrangement
Mean of measured / simulated cells and area between minimum and maximum temperature

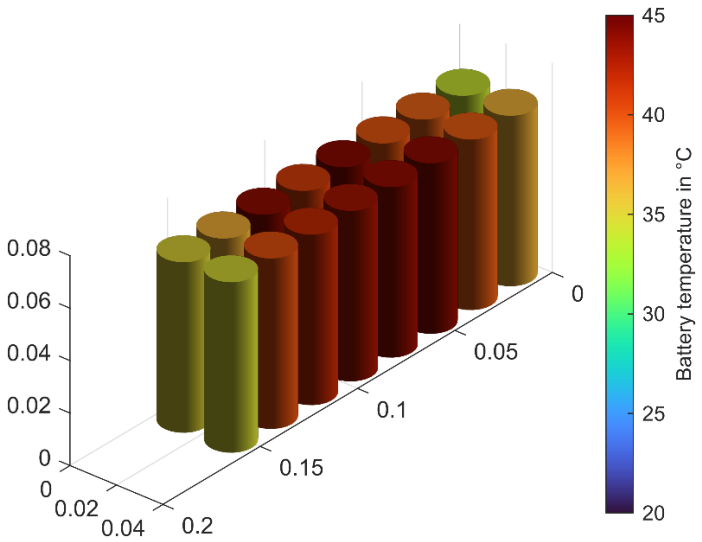

Figure 12: 4s4p module under cyclic load at temperature maximum (generated with Simscape Battery)
Peak temperature in the center of the module, temperature delta of 9.7 °C between coldest and hottest cell

4 Discussion

The starting point for the battery cell model is the electrical sub model. In this study, an ECM is utilized and the number of RC elements is set to two. The results of the investigations show that using only one RC element leads to relatively large errors (12.84 mV) when numerically fitting the voltage response during the pulses to the measurement. Increasing the number to two RC elements significantly reduces the fitting error to a maximum of 1.63 mV. However, further increasing the number to four RC elements does not provide any substantial improvement but instead results in significantly increased model complexity.

To achieve higher accuracy in the model, it is essential to ensure that the smallest RC time constant is greater than the maximum simulation step size. For four RC elements, this time constant is 0.1483 s, which requires a correspondingly small maximum time step in the simulation. This, in turn, leads to a significant increase in simulation duration. The studies by Baumann [35] and Reiter [35] confirm that an ECM with two RC elements represents the optimal compromise between accuracy and computational effort.

The validation of the thermal model is done on system level and discussed later on. The determined value for the specific heat capacity is 927.5 J kg^{-1} K^{-1}, which falls within the range specified by Steinhardt et al. [41] for the LG MJ1 cell (909–968 J kg^{-1} K^{-1}). However, this method is subject to uncertainty as the calculation

of power loss strongly depends on the resolution of the battery test device, as the alternating current generates a dynamic voltage signal that must be averaged to determine the power loss.

The aging behavior is validated on cell level only as the lifetime tests on system level are still ongoing. The SEAMs struggle to reproduce the aging trajectory of the chosen test as they are unable to capture the knee point at 800 EFC. Nonetheless, the accuracy is sufficient with an MAPE below 2 % until 80 % SoH and below 6 % until the end of the test – which is at a lower SoH than typically reached in real-world usage.

The validation on system level includes the electrical and thermal validation on single cell level. It demonstrates the ability of the proposed model to reproduce the electrical behavior of the investigated systems with high accuracy as indicated by an MAPE below 1 % for all systems. This also holds true for the cell level, as errors cumulate on system level and are lower at cell level without further quantification at this point. The thermal precision of the model is slightly lower compared to the electrical but fulfills the requirements nevertheless with MAPEs around 5 % resulting in absolute errors of 2 °C.

5 Conclusion and Outlook

The operating conditions of a battery, among other factors, determine its aging behavior. As the conditions differ from cell to cell in battery systems (e.g., different temperature boundary conditions, cell-to-cell variations, and varying contact resistances), lifetime experiments on cell level only are insufficient. However, aging tests on system level are time-consuming and cost-expensive. Therefore, complementary simulations on system level are desirable. In this work, a modular system model including an equivalent circuit model and a lumped thermal model with an integrated semi-empirical aging model was developed. The electrical and thermal models are validated on system level. The achieved accuracy is sufficient for the analysis of thermal gradients and the divergence of cell states within battery systems. The aging model is validated on cell level, as the experimental aging experiments are still ongoing.

The transferability to other systems depends on the cell format used and the system properties: depending on the cell format, the influence varies with regard to the electrical, thermal and mechanical boundary conditions. In particular, the latter should not be neglected for systems with prismatic and pouch cells, since the pressure during operation is not constant and increases with aging. In addition, it can be assumed that scaling from the cell to the system level is only possible to a limited extent if a significant heat flow is supplied or removed via a cooling system at the system level, provided that this was not implemented comparably during the characterization and aging of the individual cells. Further investigations must be carried out – both simulative and experimental – to verify the transferability to other systems.

The next steps include finalizing the aging study on system level for all six modules, analyzing the differences between the aging behavior on cell and system level as well as validating the aging model on system level. Based on these results, the ability of this concept to reduce testing effort at the system level can be evaluated.

Acknowledgments

The authors greatly acknowledge the funding of the Bavarian State Ministry of Economic Affairs, Regional Development and Energy within "TwinBat" under the grant number DIK0564/02.
We thank TUM.Battery for promoting battery research by providing an interdisciplinary network of experts.

References

[1] M. H. Hossain, M. A. Chowdhury, N. Hossain, M. A. Islam, and M. H. Mobarak, "Advances of lithium-ion batteries anode materials—A review," *Chemical Engineering Journal Advances*, vol. 16, p. 100569, 2023, doi: 10.1016/j.ceja.2023.100569.

[2] S. Paarmann *et al.*, "Short-Term Tests, Long-Term Predictions – Accelerating Ageing Characterisation of Lithium-Ion Batteries," *Batteries & Supercaps*, 2024, Art. no. e202300594, doi: 10.1002/batt.202300594.

[3] T. Kröger, S. Maisel, G. Jank, K. A. Gamra, T. Brehler, and M. Lienkamp, "Comparing experimental designs for parameterizing semi-empirical and deep learning-based lithium-ion battery aging models," *Journal of Energy Storage*, vol. 106, p. 114702, 2025, doi: 10.1016/j.est.2024.114702.

[4] M. J. Brand, M. H. Hofmann, M. Steinhardt, S. F. Schuster, and A. Jossen, "Current distribution within parallel-connected battery cells," *Journal of Power Sources*, vol. 334, pp. 202–212, 2016, doi: 10.1016/j.jpowsour.2016.10.010.

[5] T. Bruen and J. Marco, "Modelling and experimental evaluation of parallel connected lithium ion cells for an electric vehicle battery system," *Journal of Power Sources*, vol. 310, pp. 91–101, 2016, doi: 10.1016/j.jpowsour.2016.01.001.
[6] A. Fill and K. P. Birke, "Interaction of Temperature and Current Differences among parallel-connected Lithium-Ion Cells in Dependency of the thermal Battery Design," in *2022 IEEE 21st Mediterranean Electrotechnical Conference (MELECON)*, Palermo, Italy, 2022, pp. 195–200, doi: 10.1109/MELECON53508.2022.9842985.
[7] R. Gogoana, M. B. Pinson, M. Z. Bazant, and S. E. Sarma, "Internal resistance matching for parallel-connected lithium-ion cells and impacts on battery pack cycle life," *Journal of Power Sources*, vol. 252, pp. 8–13, 2014, doi: 10.1016/j.jpowsour.2013.11.101.
[8] S. Miyatake, Y. Susuki, T. Hikihara, S. Itoh, and K. Tanaka, "Discharge characteristics of multicell lithium-ion battery with nonuniform cells," *Journal of Power Sources*, vol. 241, pp. 736–743, 2013, doi: 10.1016/j.jpowsour.2013.05.179.
[9] M. H. Hofmann *et al.*, "Dynamics of current distribution within battery cells connected in parallel," *Journal of Energy Storage*, vol. 20, pp. 120–133, 2018, doi: 10.1016/j.est.2018.08.013.
[10] E. Hosseinzadeh *et al.*, "Quantifying cell-to-cell variations of a parallel battery module for different pack configurations," *Applied Energy*, vol. 282, p. 115859, 2021, doi: 10.1016/j.apenergy.2020.115859.
[11] X. Liu, W. Ai, M. Naylor Marlow, Y. Patel, and B. Wu, "The effect of cell-to-cell variations and thermal gradients on the performance and degradation of lithium-ion battery packs," *Applied Energy*, vol. 248, pp. 489–499, 2019, doi: 10.1016/j.apenergy.2019.04.108.
[12] K. Rumpf, A. Rheinfeld, M. Schindler, J. Keil, T. Schua, and A. Jossen, "Influence of Cell-to-Cell Variations on the Inhomogeneity of Lithium-Ion Battery Modules," *J. Electrochem. Soc.*, vol. 165, no. 11, A2587-A2607, 2018, doi: 10.1149/2.0111811jes.
[13] M. Schindler, P. Jocher, A. Durdel, and A. Jossen, "Analyzing the Aging Behavior of Lithium-Ion Cells Connected in Parallel Considering Varying Charging Profiles and Initial Cell-to-Cell Variations," *J. Electrochem. Soc.*, vol. 168, no. 9, p. 90524, 2021, doi: 10.1149/1945-7111/ac2089.
[14] G. J. Offer, V. Yufit, D. A. Howey, B. Wu, and N. P. Brandon, "Module design and fault diagnosis in electric vehicle batteries," *Journal of Power Sources*, vol. 206, pp. 383–392, 2012, doi: 10.1016/j.jpowsour.2012.01.087.
[15] B. Wu, V. Yufit, M. Marinescu, G. J. Offer, R. F. Martinez-Botas, and N. P. Brandon, "Coupled thermal–electrochemical modelling of uneven heat generation in lithium-ion battery packs," *Journal of Power Sources*, vol. 243, pp. 544–554, 2013, doi: 10.1016/j.jpowsour.2013.05.164.
[16] L. Chang *et al.*, "Influence of the Assembly Method on the Cell Current Distribution of Series–Parallel Battery Packs Based on Connector Resistance," *Front. Energy Res.*, vol. 10, 2022, Art. no. 804303, doi: 10.3389/fenrg.2022.804303.
[17] E. Hosseinzadeh, J. Marco, and P. Jennings, "Combined electrical and electrochemical-thermal model of parallel connected large format pouch cells," *Journal of Energy Storage*, vol. 22, pp. 194–207, 2019, doi: 10.1016/j.est.2019.02.004.
[18] R. Luca *et al.*, "Current Imbalance in Parallel Battery Strings Measured Using a Hall-Effect Sensor Array," *Energy Tech*, vol. 9, no. 4, 2021, Art. no. 2001014, doi: 10.1002/ente.202001014.
[19] M. Schindler, A. Durdel, J. Sturm, P. Jocher, and A. Jossen, "On the Impact of Internal Cross-Linking and Connection Properties on the Current Distribution in Lithium-Ion Battery Modules," *J. Electrochem. Soc.*, vol. 167, no. 12, p. 120542, 2020, doi: 10.1149/1945-7111/abad6b.
[20] Y. Zhang *et al.*, "Nonuniform current distribution within parallel-connected batteries," *Int J Energy Res*, vol. 42, no. 8, pp. 2835–2844, 2018, doi: 10.1002/er.4039.
[21] H. He, A. Fly, E. Barbour, and X. Chen, "Numerical investigation of module-level inhomogeneous ageing in lithium-ion batteries from temperature gradients and electrical connection topologies," *Commun Eng*, vol. 3, no. 1, 2024, doi: 10.1038/s44172-024-00222-3.
[22] I. Zilberman, S. Ludwig, M. Schiller, and A. Jossen, "Online aging determination in lithium-ion battery module with forced temperature gradient," *Journal of Energy Storage*, vol. 28, p. 101170, 2020, doi: 10.1016/j.est.2019.101170.
[23] J. N. E. Lucero, V. A. Sujan, and S. Onori, "An experimentally validated electro-thermal EV battery pack model incorporating cycle-life aging and cell-to-cell variations," *IEEE Trans. Transp. Electrific.*, p. 1, 2024, doi: 10.1109/TTE.2024.3365028.
[24] A. Cordoba-Arenas, S. Onori, and G. Rizzoni, "A control-oriented lithium-ion battery pack model for plug-in hybrid electric vehicle cycle-life studies and system design with consideration of health management," *Journal of Power Sources*, vol. 279, pp. 791–808, 2015, doi: 10.1016/j.jpowsour.2014.12.048.
[25] C. Escobar, Z. Gong, C. Da Silva, O. Trescases, and C. H. Amon, "Effect of Cell-to-Cell Thermal Imbalance and Cooling Strategy on Electric Vehicle Battery Performance and Longevity," in *Proceedings of the Twenty First InterSociety Conference on Thermal and Thermomechanical Phenomena in Electronic Systems: ITherm 2022 : May 31-June 3, 2022, San Diego, CA, USA*, San Diego, CA, USA, 2022, pp. 1–9, doi:

10.1109/iTherm54085.2022.9899683.
[26] G. Gálik, M. M. Uličný, Š. Berta, and J. Paulech, "System model of battery module using computational fluid dynamics thermal analysis," in *Applied Physics Of Condensed Matter 2024*, p. 60006.
[27] J. Jaguemont, L. Boulon, and Y. Dube, "Characterization and Modeling of a Hybrid-Electric-Vehicle Lithium-Ion Battery Pack at Low Temperatures," *IEEE Trans. Veh. Technol.*, vol. 65, no. 1, pp. 1–14, 2016, doi: 10.1109/TVT.2015.2391053.
[28] M. Kolmbauer, G. Offner, R. U. Pfau, and B. Pöchtrager, "Battery Module Simulation Based on Model Exchange FMU Cell Models and Its Application in Multi-physical System Simulation Software," in *Scientific computing in electrical engineering: SCEE 2022, Amsterdam, The Netherlands, July 2022* (Mathematics in Industry The European Consortium for Mathematics in Industry 43), M. C. van Beurden, N. V. Budko, G. Ciuprina, W. Schilders, H. Bansal, and R. Barbulescu, Eds., Cham: Springer Nature Switzerland; Imprint Springer, 2024, pp. 201–207.
[29] J. He, M. Sazzad Hosen, R. Youssef, T. Kalogiannis, J. van Mierlo, and M. Berecibar, "A lumped electro-thermal model for a battery module with a novel hybrid cooling system," *Applied Thermal Engineering*, vol. 221, p. 119874, 2023, doi: 10.1016/j.applthermaleng.2022.119874.
[30] S. Neupert and J. Kowal, "Inhomogeneities in Battery Packs," *WEVJ*, vol. 9, no. 2, p. 20, 2018, doi: 10.3390/wevj9020020.
[31] C. Reiter, L. Wildfeuer, N. Wassiliadis, T. Krahl, J. Dirnecker, and M. Lienkamp, "A Holistic Approach for Simulation and Evaluation of Electrical and Thermal Loads in Lithium-Ion Battery Systems," in *2019 Fourteenth International Conference on Ecological Vehicles and Renewable Energies (EVER)*, Monte-Carlo, Monaco, 2019, pp. 1–17, doi: 10.1109/EVER.2019.8813640.
[32] M. Elmahallawy, T. Elfouly, A. Alouani, and A. M. Massoud, "A Comprehensive Review of Lithium-Ion Batteries Modeling, and State of Health and Remaining Useful Lifetime Prediction," *IEEE Access*, vol. 10, pp. 119040–119070, 2022, doi: 10.1109/ACCESS.2022.3221137.
[33] *Simscape Battery* (2024). The MathWorks Inc. Accessed: Mar. 14, 2025. [Online]. Available: https://de.mathworks.com/help/simscape-battery/
[34] G. L. Plett, *Battery management systems: Volume 1: battery modeling* (Artech House power engineering and power electronics). Boston, London: Artech House, 2015.
[35] M. Baumann, "Methode zur Parameterbestimmung und -prädiktion von Lithium-Ionen-Traktionsbatterien," Dissertation, Institute of Automotive Technology, Technical University of Munich, Munich, 2019.
[36] W. Zhao, M. Rohde, I. U. Mohsin, C. Ziebert, and H. J. Seifert, "Heat Generation in NMC622 Coin Cells during Electrochemical Cycling: Separation of Reversible and Irreversible Heat Effects," *Batteries*, vol. 6, no. 4, p. 55, 2020, doi: 10.3390/batteries6040055.
[37] T. S. Bryden *et al.*, "Methodology to determine the heat capacity of lithium-ion cells," *Journal of Power Sources*, vol. 395, pp. 369–378, 2018, doi: 10.1016/j.jpowsour.2018.05.084.
[38] M. Ank, T. Brehler, and M. Lienkamp, "Wire bond contact defect identification in battery modules of electric vehicles using pulses and differential voltage analysis," *eTransportation*, vol. 18, p. 100284, 2023, doi: 10.1016/j.etran.2023.100284.
[39] S. F. Schuster, M. J. Brand, P. Berg, M. Gleissenberger, and A. Jossen, "Lithium-ion cell-to-cell variation during battery electric vehicle operation," *Journal of Power Sources*, vol. 297, pp. 242–251, 2015, doi: 10.1016/j.jpowsour.2015.08.001.
[40] P. Jocher, M. Steinhardt, S. Ludwig, M. Schindler, J. Martin, and A. Jossen, "A novel measurement technique for parallel-connected lithium-ion cells with controllable interconnection resistance," *Journal of Power Sources*, vol. 503, p. 230030, 2021, doi: 10.1016/j.jpowsour.2021.230030.
[41] M. Steinhardt *et al.*, "Low-effort determination of heat capacity and thermal conductivity for cylindrical 18650 and 21700 lithium-ion cells," *Journal of Energy Storage*, vol. 42, p. 103065, 2021, doi: 10.1016/j.est.2021.103065.

Presenter Biography

Tobias Brehler received his bachelor's in mechanical engineering and master's in automotive technology, focusing on battery electric vehicles, from the Technical University of Munich (TUM) in 2020 and 2023. In 2024, he received his master's in business administration from the Collège des Ingénieurs (CDI) in Paris. He is currently pursuing a Ph.D. degree at the Institute of Automotive Technology at the TUM, where his research focuses on the aging and modeling of Li-ion batteries at system level.